JOURNAL OF CHEMICAL & ENGINEERING DATA

ARTICLE

pubs.acs.org/jced

Thermodynamic Functions of $PrBr_3$ and Congruently Melting M_3PrBr_6 Compounds (M = K, Rb, Cs)

L. Rycerz,[†] I. Chojnacka,[†] M. Berkani,[‡] and M. Gaune-Escard*[,§]

[†]Chemical Metallurgy Group, Faculty of Chemistry, Wroclaw University of Technology, Wybrzeze Wyspianskiego 27, 50-370 Wroclaw, Poland

[‡]Laboratoire des Procédés Catalytiques et Thermodynamique des Matériaux, Département de Génie des Procédés, Faculté des Sciences et des Sciences de l'Ingénieur, Université A. Mira de Béjaïa, 06000 Béjaïa, Algérie

[§]Polytech Marseille, Laboratoire IUSTI, CNRS-UMR 6595, Mecanique Energetique, Technopole de Chateau-Gombert, 5 rue Enrico Fermi, 13453 Marseille Cedex 13, France

ABSTRACT: The temperatures and enthalpies of phase transitions as well as the heat capacity of solid and liquid $PrBr_3$, K_3PrBr_6, Rb_3PrBr_6, and Cs_3PrBr_6 were measured by differential scanning calorimetry in the temperature range from 400 K up to 1100 K. A linear heat capacity dependence on temperature was used to fit the experimental data. Through a combination of these experimental results with the entropy at 298.15 K, the thermodynamic functions of $PrBr_3$ and M_3PrBr_6 compounds were calculated up to T = 1100 K.

INTRODUCTION

Rare earth bromides and iodides are attractive components for doses in high-intensity discharge lamps[1,2] and new highly efficient light sources with energy saving features.[3] They offer the opportunity when combined with other metal halides to design light sources with high efficacy and good color rendition. Photoluminescence and photostimulated luminescence of lanthanide-doped bromide materials induced recently active research targeted to commercial X-ray storage phosphors.[4] There is also a continued interest in the search for new scintillators for the detection of radiation.[5−7] Lanthanide trihalides LnX_3, (pseudo)-elpasolites M_2ALnX_6, and ternary halides $A_mLn_nX_o$ have been investigated recently in this respect.[7]

However, in spite of their technological interest, the properties of many rare earth halides are still poorly characterized. The bromides have received even less attention in the scientific literature than the chlorides and iodides. Comprehensive thermochemical parameters for the lanthanide tribromides are not available in any of the standard compilations of thermodynamic properties. These properties are required for example for the chemical composition calculation in discharge lamps to assist in the understanding and hence to help with tungsten corrosion, silica corrosion, and spectral output issues. Data are also needed for predicting the behavior of doses by modeling multicomponent metal halide systems. Therefore, it is clear that more details are required to fully characterize those systems. In view of the above reasons or lack of data for many $LnBr_3$-based binary systems, we decided to assess existing data and to investigate the still unexplored lanthanide bromide-based systems. We have determined previously phase diagrams of praseodymium(III) bromide-alkali metal bromide binary systems (alkali metal = Li, Na, K, Rb, Cs).[8−11] The congruently melting M_3PrBr_6 compounds were found in the systems with M = K, Rb, and Cs.[9−11]

The present work reports experimental thermodynamic properties (temperatures and enthalpies of phase transitions as well as heat capacity ($C^0_{p,m}$)) of $PrBr_3$ and of the above-mentioned M_3PrBr_6 compounds.

EXPERIMENTAL SECTION

Chemicals. Praseodymium(III) bromide was synthesized from the praseodymium oxide, Pr_6O_{11}. This oxide was dissolved in hot concentrated HBr acid. The solution was evaporated, and $PrBr_3 \cdot xH_2O$ was crystallized. Ammonium bromide was then added, and this wet mixture of hydrated $PrBr_3$ and NH_4Br was first slowly heated up to 450 K and then up to 570 K to remove the water. The resulting mixture was subsequently heated to 650 K for sublimation of NH_4Br. Finally, the salt was melted at about 1100 K. Crude $PrBr_3$ was purified by distillation under reduced pressure (~0.1 Pa) in a quartz ampule at 1150 K. $PrBr_3$ prepared in this way was of a high purity—minimum 99.9 %. Chemical analysis was performed by mercurimetric (bromine) and complexometric (praseodymium) methods. The results were as follows: Pr, 36.96 ± 0.15 % (37.02 % theoretical); Br, 63.04 ± 0.11 % (62.98 % theoretical).

Potassium, rubidium, and cesium bromides were Merck Suprapur reagent (minimum 99.9 %). Before use, they were progressively heated up to fusion under gaseous HBr atmosphere. Excess HBr was then removed from the melt by argon bubbling.

All chemicals were handled inside a glovebox with high purity argon atmosphere.

Stoichiometric M_3PrBr_6compounds (M = K, Rb, Cs) were prepared from $PrBr_3$ and appropriate MBr, which were weighed in the molar ratio 1:3. All of the mixtures were prepared in a

Special Issue: John M. Prausnitz Festschrift

Received: October 29, 2010
Accepted: February 17, 2011
Published: March 11, 2011

glovebox filled with purified and water-free argon. Although only a small amount of samples were used for the differential scanning calorimetry (DSC) experiments ((300 to 500) mg), several grams of each compound were synthesized to avoid deviations from stoichiometry. Stoichiometric mixtures of bromides were melted in vacuum-sealed quartz ampules in an electric furnace. Melts were homogenized by shaking and solidified. These samples were ground in an agate mortar in a glovebox. All chemicals were handled in an argon glovebox with a measured volume fraction of water of about $2 \cdot 10^{-6}$ and continuous gas purification by forced recirculation through external molecular sieves.

Measurements. The temperatures and enthalpies of the phase transitions were measured with a Setaram DSC 121 differential scanning calorimeter. The apparatus and the measurement procedure have been described in detail previously.[12,13] Samples of (300 to 500) mg were contained in quartz ampules (about 6 mm diameter, 15 mm length) sealed under a reduced pressure of argon. The sidewalls of the ampules were grounded to fit the cells snugly into the heat flow detector. Experiments were conducted at heating and cooling rates of 5 $K \cdot min^{-1}$. The integration of peaks area related to the thermal effects was made by Setaram software. Temperatures of the effects (formation, transition, fusion) were determined as onset temperatures.

The heat capacity was measured with the same Setaram DSC 121 operated in a stepwise mode. This so-called "step method" has already been described.[13−17] The heat capacity of the sample was determined over an extended temperature range from two experimental runs in an identical stepwise mode. The first one was registered with two empty cells (containers) of identical mass and the second with one of these cells loaded with the sample. For each heating step, the difference of heat flux between the two series is proportional to the amount of heat (Q_i) necessary to increase the sample temperature by a small temperature increment ΔT_i. Therefore, in the absence of any phase transition, the heat capacity of the sample is equal to:

$$C_{p,m} = (Q_i \cdot M_s)/(\Delta T_i \cdot m_s) \quad (1)$$

where m_s is the mass of the sample and M_s is the molar mass of the sample.

The same operating conditions (i.e., initial and final temperatures, temperature increment, isothermal delay, and heating rate) were used in the two experimental series. Experimental monitoring, data acquisition, and processing were performed with the Setaram Setsys software.

The DSC 121 apparatus was calibrated by the Joule effect, and some test measurements were performed separately with NIST 720 α-Al_2O_3 Standard Reference material prior to investigation. These tests resulted in $C_{p,m}$ values consistent with standard data for Al_2O_3 (difference less than 1.5 %), with an exception in the temperature range (300 to 400) K, in which the measured values were significantly larger. Results of measurements in this temperature range were not taken into account in the polynomial fitting of experimental results.

In the present heat capacity experiments each 5 K heating step was followed by a 400 s isothermal delay. The heating rate was 1.5 $K \cdot min^{-1}$. All experiments were performed in the (400 to 1100) K temperature range. The mass difference of the quartz cells in any individual experiment did not exceed 1 mg (cell mass: (400 to 500) mg).

To establish the repeatability and uncertainty of the results, three different samples of each compound (from different batches) were used in measurements. All of these results were used in the calculation of coefficients in the equation describing the temperature dependence of heat capacity as well as the standard deviation on $C^0_{p,m}$. The maximal deviations of individual series from mean values did not exceed ± 3 %.

Table 1. Temperatures and Molar Enthalpies of Phase Transitions of $PrBr_3$ and Congruently Melting M_3PrBr_6 Compounds (M = K, Rb, Cs)

	T_{form}	$\Delta_{form}H_m$	T_{trs}	$\Delta_{trs}H_m$	T_{fus}	$\Delta_{fus}H_m$
compound	K	$kJ \cdot mol^{-1}$	K	$kJ \cdot mol^{-1}$	K	$kJ \cdot mol^{-1}$
$PrBr_3$	-	-	-	-	960	46.40 ± 0.60
K_3PrBr_6	727	46.10 ± 0.55	-	-	904	39.600 ± 0.63
Rb_3PrBr_6	*a*	*a*	704	7.50 ± 0.15	983	49.72 ± 0.31
Cs_3PrBr_6	-	-	726	8.37 ± 0.17	1051	58.22 ± 0.76

[a] Not determined because of metastable phase formation. Instead an additional effect at 394 K with related enthalpy of 0.59 $kJ \cdot mol^{-1}$ was observed.

All of the results obtained are presented with two decimals. Three decimals (with no physical meaning) in the presentation of thermodynamic functions are recommended by the CODATA Task Group on Chemical Thermodynamic Tables.[18] Most of the tables[19,20] are in accordance with this recommendation. The thermodynamic tables prepared by Kubaschewski and co-workers[21] give heat capacity data with two decimals. In the present work, this last way of data presentation was adopted.

RESULTS AND DISCUSSION

Temperature and Enthalpy of Phase Transitions. The experimental temperatures and enthalpies of phase transitions are presented in Table 1 for $PrBr_3$, K_3PrBr_6, Rb_3PrBr_6, and Cs_3PrBr_6. Our experimental fusion temperature and fusion enthalpy for $PrBr_3$ obtained by differential scanning calorimetry could be compared with Dworkin and Bredig[22] values (966 K, 47.3 $kJ \cdot mol^{-1}$, respectively) obtained by drop calorimetry. Very good agreement was found for the fusion enthalpy (46.40 $kJ \cdot mol^{-1}$), whereas our experimental fusion temperature is slightly lower (960 K).

The results on K_3PrBr_6, Rb_3PrBr_6, and Cs_3PrBr_6 could be compared only with our preliminary results which have been obtained in the course of phase diagram determination.[9−11] They have now been verified and completed by DSC measurements performed on samples from three different batches prepared in the scale of several grams (to minimize deviation from stoichiometry). No other data on these compounds were found in literature.

As discussed in detail previously[9] K_3PrBr_6 forms at 727 K from KBr and K_2PrBr_5 and melts congruently at 904 K. The molar enthalpy related to this effect, $\Delta_{form}H_m$ = 46.1 $kJ \cdot mol^{-1}$, is in excellent agreement with the enthalpy observed for the formation of many M_3LnX_6 compounds (M = K, Rb; Ln = lanthanide) by reaction between MX and M_2LnX_5 ((45 to 55) $kJ \cdot mol^{-1}$).[14]

It was found previously[10] that Rb_3PrBr_6 undergoes a solid−solid phase transition at 704 K with the enthalpy 8.0 $kJ \cdot mol^{-1}$. Actual measurements gave the temperature and enthalpy of this transition as 704 K and 7.5 $kJ \cdot mol^{-1}$ and congruent melting at 983 K, respectively. The enthalpy magnitude is comparable to that of solid−solid phase transition in several M_3LnX_6 compounds (M = Rb, Cs; Ln = lanthanide).[14]

By analogy to other M_3LnX_6 compounds (M = K, Rb) one could expect the formation of Rb_3PrBr_6 from Rb_2PrBr_5 and RbBr

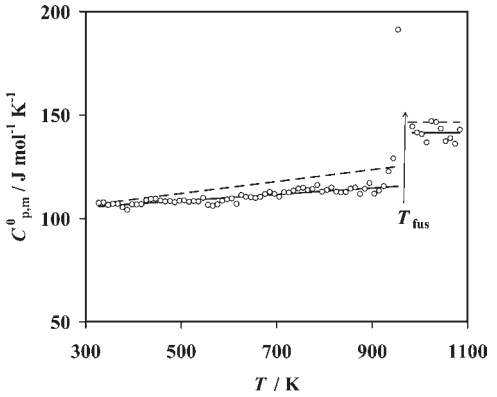

Figure 1. Molar heat capacity $C^0_{p,m}$ of $PrBr_3$: open circles, experimental results; solid lines, linear fitting of experimental results; broken lines, Pankratz[20] data.

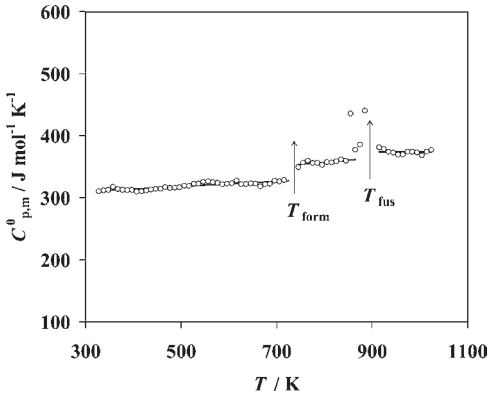

Figure 2. Molar heat capacity $C^0_{p,m}$ of K_3PrBr_6: open circles, experimental results; solid lines, linear fitting of experimental results.

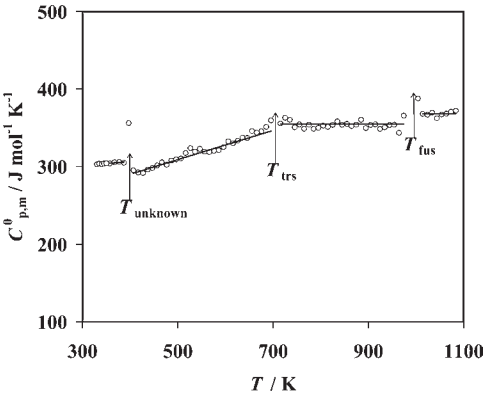

Figure 3. Molar heat capacity $C^0_{p,m}$ of Rb_3PrBr_6: open circles, experimental results; solid lines, linear fitting of experimental results.

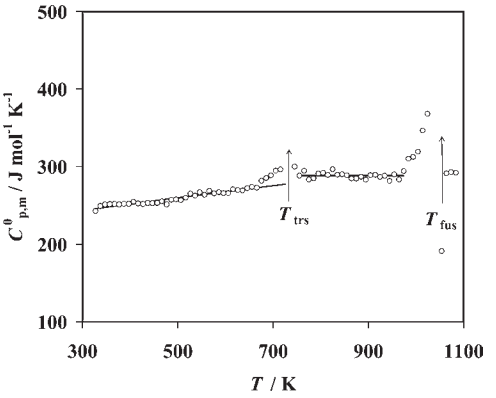

Figure 4. Molar heat capacity $C^0_{p,m}$ of Cs_3PrBr_6: open circles, experimental results; solid lines, linear fitting of experimental results.

at higher temperatures. However such a formation should be associated to large enthalpy changes ((45 to 55) kJ·mol^{-1}).[14] Additional DSC experiments performed on Rb_3PrBr_6 did not show any thermal effect of such a magnitude. Each time a smaller thermal effect with related enthalpy 7.50 kJ·mol^{-1} was measured instead. In addition a very small endothermic effect appeared at 394 K. It is very likely that Rb_3PrBr_6 does not decompose upon cooling and that a metastable phase of this compound is formed instead. Such behavior has been addressed in literature for many M_3LnCl_6 chloride compounds, and it has been postulated that those compounds that form at temperatures below 700 K may exist as a metastable phase at lower temperatures.[23] A solid-state reaction is a special kind of reconstructive phase transition in which the arrangement of the ions is drastically changed in the structures surrounding this transition. Ions have to move from one site to another passing strong potential walls of other ions. The resulting "kinetic hindrance" can cause great difference between the reaction temperatures measured in DSC heating and cooling runs (thermal hysteresis). In extreme cases during cooling experiments, the "undercooling" can become so strong that the reaction does not occur in the DSC time-scale. Because of kinetic reasons, the decomposition during cooling does not occur, and the compound still exists in a metastable form. This metastability was observed for several M_3LnX_6 compounds (Rb_3PrCl_6, Rb_3NdCl_6, K_3TbCl_6, K_3TbBr_6),[14] and no decomposition was detected during cooling runs.

A similar situation probably takes place in the case of the Rb_3PrBr_6 compound. The small molar enthalpy related to the effect at 704 K confirms that it is not formation, but a solid−solid phase transition. As a nonreconstructive phase transition, it is associated with a small molar enthalpy (7.50 kJ·mol^{-1}). The additional effect of unknown origin at 394 K with enthalpy of about 0.6 kJ·mol^{-1} is probably the aforementioned metastable phase.

The compound with cesium, Cs_3PrBr_6, is stable or metastable at ambient temperature. It undergoes a solid−solid state phase transition at 726 K and melts congruently at 1051 K with the related enthalpies (8.4 and 58.2) kJ·mol^{-1}, respectively.

Heat Capacity. Experimental heat capacity data (mean values from measurements performed on three different samples) on $PrBr_3$, K_3PrBr_6, Rb_3PrBr_6, and Cs_3PrBr_6 are plotted against temperature in Figures 1 to 4. As the results on M_3PrBr_6 compounds were obtained for the first time during this work, only those corresponding to $PrBr_3$ could be compared with literature data.

We found that the heat capacity of solid $PrBr_3$ (Figure 1) varies linearly with temperature. The heat capacity estimated by Pankratz[20] is larger in the whole temperature range. This difference increases with temperature (from about 1 % at 350 K, through 5.5 % at 700 K, and up to 7.5 % at 900 K). A constant heat capacity value, $C^0_{p,m}$ = 141.38 ± 3.67 J·mol^{-1}·K^{-1}, was found for liquid $PrBr_3$. This value is smaller by 9 % than that given by Pankratz.[20]

Heat capacity dependence on temperature of the M_3PrBr_6 compounds (M = Rb, Cs) is presented in Figures 2 to 4.

dx.doi.org/10.1021/je101139k |J. Chem. Eng. Data 2011, 56, 1293–1298

Table 2. Thermodynamic Functions of $PrBr_3$ and M_3PrBr_6: Values of *A*, *B*, *C*, *D*, and *E* Parameters in eqs 2 to 5

	temp. range	*A*	$B \cdot 10^2$	$C \cdot 10^{-3}$	*D*	*E*
compound	K	$J \cdot mol^{-1} \cdot K^{-1}$	$J \cdot mol^{-1} \cdot K^{-2}$	$J \cdot mol^{-1}$	$J \cdot mol^{-1} \cdot K^{-1}$	$J \cdot mol^{-1} \cdot K^{-1}$
$PrBr_{3(s)}$	298−960	100.80 ± 0.70	1.531 ± 0.107	−30.730 ± 0.260	−386.42 ± 4.31	−487.21 ± 5.01
$PrBr_{3(l)}$	960−1100	141.38 ± 3.67	-	−16.240 ± 2.610	−602.084 ± 23.67	−743.46 ± 24.61
$K_3PrBr_{6(s)}$	298−727	297.28 ± 2.16	4.122 ± 0.405	−90.471 ± 0.820	−1220.76 ± 13.52	−1518.06 ± 12.91
$K_3PrBr_{6(s)}$	727−904	304.82 ± 21.54	6.525 ± 2.707	−56.200 ± 21.000	−1224.52 ± 157.89	−1529.36 ± 177.85
$K_3CeBr_{6(l)}$	904−1100	373.76 ± 3.64	-	−52.260 ± 6.250	−1591.02 ± 11.54	−1964.78 ± 27.44
$Rb_3PrBr_{6(s)}$	298−394	287.11 ± 3.53	4.810 ± 0.996	−87.740 ± 1.502	−1126.54 ± 23.09	−1413.59 ± 26.64
$Rb_3PrBr_{6(s)}$	394−704	214.61 ± 14.42	18.854 ± 3.222	−69.574 ± 7.520	−747.25 ± 96.94	−961.83 ± 111.37
$Rb_3PrBr_{6(s)}$	704−983	354.71 ± 7.68	-	−11.398 ± 0.521	−1522.48 ± 32.34	−1731.47 ± 63.89
$Rb_3PrBr_{6(l)}$	983−1100	368.02 ± 2.73	-	−77.360 ± 10.070	−1563.63 ± 4.05	−1890.29 ± 21.49
$Cs_3PrBr_{6(s)}$	298−726	220.54 ± 2.91	7.813 ± 0.567	−69.230 ± 1.120	−730.04 ± 18.27	−950.59 ± 21.19
$Cs_3PrBr_{6(s)}$	726−1051	288.19 ± 5.77	-	−89.380 ± 1.710	−1107.44 ± 32.99	−1395.63 ± 38.78
$Cs_3PrBr_{6(l)}$	1051−1100	291.99 ± 0.84	-	−35.152 ± 03.470	−1077.49 ± 3.45	−1370.47 ± 4.21

Table 3. Thermodynamic Functions of $PrBr_3$ at Selected Temperatures (from (298.15 to 1100) K)

T	$C_{p,m}^0(T)$	$S_m^0(T)$	$-(G_m^0(T) - H_m^0(298.15\ K))/T$	$H_m^0(T) - H_m^0(298.15\ K)$
K	$J \cdot mol^{-1} \cdot K^{-1}$	$J \cdot mol^{-1} \cdot K^{-1}$	$J \cdot mol^{-1} \cdot K^{-1}$	$kJ \cdot mol^{-1}$
298.15	105.37	192.46	192.46	0.00
300	105.39	193.12	192.46	0.20
331	105.87	203.50	193.02	3.47
400	106.93	223.64	196.62	10.82
500	108.46	247.67	204.51	21.58
600	109.99	267.58	213.41	32.51
700	111.52	284.65	222.40	43.58
800	113.05	299.64	231.14	54.81
900	114.58	313.04	239.51	66.19
960	115.50	320.47	244.34	73.09
960	141.39	368.80	244.34	119.49
1000	141.39	374.57	249.43	125.15
1065	141.39	383.48	257.35	134.34
1100	141.39	388.05	261.43	139.28

Table 4. Thermodynamic Functions of K_3PrBr_6 at Selected Temperatures (from (298.15 to 1100) K)

T	$C_{p,m}^0(T)$	$S_m^0(T)$	$-(G_m^0(T) - H_m^0(298.15\ K))/T$	$H_m^0(T) - H_m^0(298.15\ K)$
K	$J \cdot mol^{-1} \cdot K^{-1}$	$J \cdot mol^{-1} \cdot K^{-1}$	$J \cdot mol^{-1} \cdot K^{-1}$	$kJ \cdot mol^{-1}$
298.15	309.57	485.30	485.30	0.00
300	309.64	487.21	485.30	0.57
400	313.77	576.85	497.49	31.74
500	317.89	647.31	520.66	63.32
600	322.01	705.63	546.76	95.32
700	326.13	755.58	573.11	127.72
727	327.25	767.95	580.11	136.54
727	352.26	831.35	580.11	182.65
800	357.02	865.28	604.60	208.54
900	363.55	907.71	635.96	244.56
904	363.81	909.33	637.17	246.02
904	373.76	953.12	637.17	285.62
1000	373.76	990.84	669.34	321.50
1100	373.76	1026.47	700.22	358.88

dx.doi.org/10.1021/je101139k |*J. Chem. Eng. Data* 2011, 56, 1293–1298

Table 5. Thermodynamic Functions of Rb_3PrBr_6 at Selected Temperatures (from (298.15 to 1100) K)

T	$C_{p,m}{}^0(T)$	$S^0_m(T)$	$-(G^0_m(T) - H^0_m(298.15\ K))/T$	$H^0_m(T) - H^0_m(298.15\ K)$
K	$J\cdot mol^{-1}\cdot K^{-1}$	$J\cdot mol^{-1}\cdot K^{-1}$	$J\cdot mol^{-1}\cdot K^{-1}$	$kJ\cdot mol^{-1}$
298.15	301.45	523.70	523.70	0.00
300	301.54	525.56	523.71	0.56
394	306.06	608.34	534.45	29.12
394	288.89	609.62	534.45	29.62
400	290.02	613.99	535.61	31.36
500	308.88	680.74	558.14	61.30
600	327.73	738.72	583.50	93.13
700	346.59	790.65	609.44	126.85
704	347.34	792.63	610.48	128.24
704	354.71	803.27	610.48	135.74
800	354.71	848.62	653.88	169.79
900	354.71	890.40	694.07	205.26
983	354.71	921.69	724.29	234.70
983	368.02	972.25	724.29	284.40
1000	368.02	978.56	729.26	290.66
1100	368.02	1013.64	757.31	327.46

Table 6. Thermodynamic Functions of Cs_3PrBr_6 at Selected Temperatures (from (298.15 to 1100) K)

T	$C_{p,m}{}^0(T)$	$S^0_m(T)$	$-(G^0_m(T) - H^0_m(298.15\ K))/T$	$H^0_m(T) - H^0_m(298.15\ K)$
K	$J\cdot mol^{-1}\cdot K^{-1}$	$J\cdot mol^{-1}\cdot K^{-1}$	$J\cdot mol^{-1}\cdot K^{-1}$	$kJ\cdot mol^{-1}$
298.15	243.83	549.80	549.80	0.00
300	243.98	551.31	549.81	0.45
400	251.79	622.57	559.47	25.24
500	259.61	679.59	577.97	50.81
600	267.42	727.62	599.01	77.16
700	275.23	769.42	620.43	104.29
726	277.26	779.50	625.95	111.47
726	288.19	791.03	625.95	119.85
800	288.19	819.00	642.53	141.17
900	288.19	852.94	664.06	169.99
1000	288.19	883.31	684.50	198.81
1051	288.19	897.64	694.49	213.51
1051	291.99	954.03	694.49	271.73
1100	291.99	967.34	706.31	286.04

A linear heat capacity dependence on temperature

$$C^0{}_{p,m}/J\cdot mol^{-1}\cdot K^{-1} = A + B\cdot(T/K) \qquad (2)$$

was used to fit experimental data. The coefficients A and B in eq 2 are listed in Table 2.

Because of the occurrence of phase transitions (formation or solid−solid transition, fusion), two or three different equations were used to account for the temperature dependence of heat capacity of solid M_3PrBr_6 compounds.

Constant heat capacity values, $C^0{}_{p,m} = 373.76 \pm 3.64\ J\cdot mol^{-1}\cdot K^{-1}$, $C^0{}_{p,m} = 368.02 \pm 2.73\ J\cdot mol^{-1}\cdot K^{-1}$, and $C^0{}_{p,m} = 291.99 \pm 0.84\ J\cdot mol^{-1}\cdot K^{-1}$ were found for liquid K_3PrBr_6, Rb_3PrBr_6, and Cs_3PrBr_6, respectively.

A wide dispersion of the heat capacity data on Cs_3PrBr_6 at temperatures just below the temperature of fusion (Figure 4) and to a lesser extent on the other compounds just below the temperature of fusion (Figure 1 to 3) was observed. It is very likely that this dispersion is caused by premelting effect. Another reason, especially for Cs_3PrBr_6, can be due to a small deviation from compound stoichiometry.

Thermodynamic Functions. For each compound in both the solid and liquid phases, the thermodynamic functions, namely, enthalpy increments $H^0{}_m(T) - H^0{}_m(298.15\ K)$ in $J\cdot mol^{-1}$, entropy $S^0{}_m(T)$, and Gibbs energy functions $-(G^0{}_m(T) - H^0{}_m(298.15))/T$ in $J\cdot mol^{-1}\cdot K^{-1}$, were calculated by using heat capacity dependence on temperature ($C^0{}_{p,m} = f(T)$). The parameters C, D, and E in eqs 3 to 5 describing enthalpy increments, entropy, and Gibbs energy functions, were calculated for each compound in the temperature range where it is solid (low and high temperature solids) or liquid. Accordingly, calculations were run by setting T equal to 298.15 and to the temperature of the solid−solid

dx.doi.org/10.1021/je101139k |J. Chem. Eng. Data 2011, 56, 1293–1298

transition, or to the temperature of fusion, respectively. They are also presented in Table 2.

$$H^0_m(T) - H^0_m(298.15) = A \cdot T + 1/2 \cdot B \cdot T^2 + C \quad (3)$$

$$S^0_m(T) = A \ln T + B \cdot T + D \quad (4)$$

$$-(G^0_m(T) - H^0_m(298.15))/T = A \ln T + 1/2 \cdot B \cdot T - C \cdot T^{-1} + E \quad (5)$$

Our experimental melting (transition) temperatures and enthalpies together with heat capacity data were used in this calculation. For all compounds, heat capacity values $C^0_{p,m}$ (s, 298.15 K) were obtained by extrapolation of experimental results to 298.15 K. The values of standard entropy at 298.15 K, also necessary in these calculations were taken from literature[20] ($PrBr_3$) or calculated by Latimer's method from anion and cation contributions.[24] These standard entropies were (192.46, 485.30, 523.70, and 549.80) $J \cdot mol^{-1} \cdot K^{-1}$ for $PrBr_3$, K_3PrBr_6, Rb_3PrBr_6, and Cs_3PrBr_6, respectively. The values of calculated thermodynamic functions at selected temperatures are presented in Tables 3 to 6.

SUMMARY

The temperatures and enthalpies of fusion as well as heat capacities of solid and liquid $PrBr_3$, K_3PrBr_6, Rb_3PrBr_6, and Cs_3PrBr_6 were determined by the DSC method. These data were used to calculate the whole set of thermodynamic functions for solid and liquid compounds.

AUTHOR INFORMATION

Corresponding Author

*Tel.: +33 491 106882. Fax: +33 491 117439. E-mail: marcelle.gaune-escard@polytech.univ-mrs.fr.

Funding Sources

Financial support by the Polish Ministry of Science and Higher Education from budget on science in 2007−2010 under the Grant No. N204 4098 33 is gratefully acknowledged.

ACKNOWLEDGMENT

L.R., I.C. and M.B. wish to thank the Ecole Polytechnique de Marseille for hospitality and support during this work.

REFERENCES

(1) Junming, T.; Bath, N. Y. *Quartz Metal Halide Lamp With Improved Lumen Maintenance.* U.S. Patent Application Publication, Pub. No. US 2008/0093993 Ai, Apr 24, 2008.

(2) Junming, T.; Bath, N. Y. *Quartz Metal Halide Lamp With Improved Lumen Maintenance*. U.S. Patent No. US 7, 786,674 B2, Aug 31, 2010.

(3) Guest, E. C.; Mucklejohn, S. A.; Preston, B.; Rouffet, J. B.; Zissis, G. "NumeLiTe": An energy effective lighting system for roadways & an industrial application of molten salts. International Symposium on Ionic Liquids. Proceedings in honour of Marcelle Gaune-Escard; Øye, H. A., Jagtoyen, A., Eds.; Carry le Rouet, France, June 26−28, 2003; pp 37−45.

(4) Gahane, D. H.; Kokode, N. S.; Muthal, P. L.; Dhopte, S. M.; Moharil, S. V. Luminescence of some Eu^{2+} activated bromides. *J. Alloys Compd.* **2009**, *484*, 660–664.

(5) Srivastava, A. M. Charge transfer transitions in the excitation spectra of PrX_3:Ce^{3+} (X = Cl, Br) scintillators. *J. Lumin.* **2009**, *129*, 17–18.

(6) Birovosuto, M. D.; Dorenbos, P.; van Eick, C. W. E.; Kramer, K. W.; Gudel, H. U. Thermal quenching of Ce^{3+} emission in PrX_3 (X = Cl, Br) by intervalence charge transfer. *J. Phys.: Condens. Matter* **2007**, *19*, 1–16.

(7) Birovosuto, M. D. Novel Gamma-Ray and Thermal Neutron Scintillators. *Search for High-Light-Yield and Fast-Response Materials*; Delft University Press: Amsterdam, 2007.

(8) Ingier-Stocka, E.; Rycerz, L.; Berkani, M.; Gaune-Escard, M. Thermodynamic and transport properties of the $PrBr_3$−MBr Binary Systems (M = Li, Na). *J. Mol. Liq.* **2009**, *148*, 40–44.

(9) Rejek, J.; Rycerz, L.; Ingier-Stocka, E.; Gaune-Escard, M. Thermodynamic and Transport Properties of the $PrBr_3$-KBr Binary System. *J. Chem. Eng. Data* **2010**, *55*, 1871–1875.

(10) Rycerz, L.; Ingier-Stocka, E.; Berkani, M.; Gaune-Escard, M. Thermodynamic and transport properties of the $PrBr_3$-RbBr binary system. *J. Alloys Compd.* **2010**, *501*, 269–274.

(11) Rycerz, L.; Ingier-Stocka, E.; Berkani, M.; Gaune-Escard, M. Phase Diagram and Electrical Conductivity of the $PrBr_3$ − CsBr Binary System. *Z. Naturforsch.* **2010**, *65a*, 859–864.

(12) Gaune-Escard, M.; Rycerz, L.; Szczepaniak, W.; Bogacz, A. Enthalpies of Phase Transition in the Lanthanide Chlorides $LaCl_3$, $CeCl_3$, $PrCl_3$, $NdCl_3$, $GdCl_3$, $DyCl_3$, $ErCl_3$ and $TmCl_3$. *J. Alloys Compd.* **1994**, *204*, 193–196.

(13) Rycerz, L.; Ingier-Stocka, E.; Cieslak-Golonka, M.; Gaune-Escard, M. Thermal and Conductometric Studies of $NdBr_3$ and $NdBr_3$-LiBr Binary System. *J. Therm. Anal. Calorim.* **2003**, *72*, 241–251.

(14) Rycerz, L. Thermochemistry of lanthanide halides and compounds formed in lanthanide halide-alkali metal halide systems (in Polish). *Scientific Papers of Institute of Inorganic Chemistry and Metallurgy of Rare Elements*; Series Monographs 35; Wroclaw University of Technology: Wroclaw, 2004.

(15) Rycerz, L.; Gaune-Escard, M. Heat Capacity of K_3LnCl_6 Compounds with Ln = La, Ce, Pr Nd. *Z. Naturforsch.* **1999**, *54a*, 229–235.

(16) Gaune-Escard, M.; Bogacz, A.; Rycerz, L.; Szczepaniak, W. Heat Capacity of $LaCl_3$, $CeCl_3$, $PrCl_3$, $NdCl_3$, $GdCl_3$, $DyCl_3$. *J. Alloys Compd.* **1996**, *235*, 176–181.

(17) Rycerz, L.; Gaune-Escard, M. Thermodynamics of $SmCl_3$ and $TmCl_3$: Experimental Enthalpy of Fusion and Heat Capacity. Estimation of Thermodynamic Functions up to 1300 K. *Z. Naturforsch.* **2002**, *57a*, 79–84.

(18) *CODATA Thermodynamic Tables*, Selection for Some Compounds of Calcium and Related Mixtures: A Prototype Set of Tables; Garvin, D., Parker, V. B., White,H. J., Eds.; Hemisphere Publishing Corporation: New York, 1987.

(19) Barin, I.; Knacke, O.; Kubaschewski, O. *Thermochemical Properties of Inorganic Substances*; Springer-Verlag: Berlin, 1977.

(20) Pankratz, L. B. Thermodynamic Properties of Halides. *U.S. Bur. Mines, Bull.* **1984**, *674*.

(21) Kubaschewski, O.; Alcock, C. B.; Spencer, P. J. *Materials Thermochemistry*, 6th ed.; Pergamon Press Ltd.: New York, 1993.

(22) Dworkin, A. S.; Bredig, M. A. Enthalpy of Lanthanide Chlorides, Bromides, and Iodides from 298−1300 K: Enthalpies of Fusion and Transition. *High Temp. Sci.* **1971**, *3* (1), 81–90.

(23) Seifert, H. J. Retarded solid state reactions III. *J. Therm. Anal. Calorim.* **1997**, *49*, 1207–1210.

(24) Spencer, P. J. Estimation of Thermodynamic Data for Metallurgical Applications. *Therm. Chim. Acta* **1998**, *314*, 1–21.